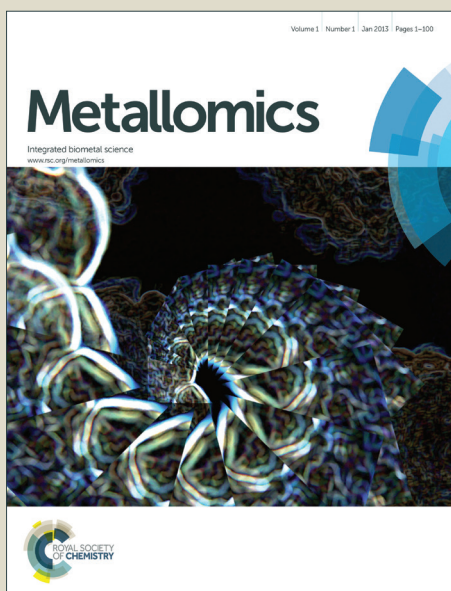


# Metallomics

Accepted Manuscript



This is an *Accepted Manuscript*, which has been through the Royal Society of Chemistry peer review process and has been accepted for publication.

*Accepted Manuscripts* are published online shortly after acceptance, before technical editing, formatting and proof reading. Using this free service, authors can make their results available to the community, in citable form, before we publish the edited article. We will replace this *Accepted Manuscript* with the edited and formatted *Advance Article* as soon as it is available.

You can find more information about *Accepted Manuscripts* in the [Information for Authors](#).

Please note that technical editing may introduce minor changes to the text and/or graphics, which may alter content. The journal's standard [Terms & Conditions](#) and the [Ethical guidelines](#) still apply. In no event shall the Royal Society of Chemistry be held responsible for any errors or omissions in this *Accepted Manuscript* or any consequences arising from the use of any information it contains.

Elemental mapping inventory of the fish *Liza aurata* brain: a biomarker of metal  
pollution vulnerability

Rita Godinho<sup>1,2,3\*</sup>, Patricia Pereira<sup>2,4,5</sup>, Joana Raimundo<sup>2,3</sup>, Mário Pacheco<sup>4</sup>, Teresa  
Pinheiro<sup>1,6</sup>

<sup>1</sup> Instituto Superior Técnico, Universidade de Lisboa, EN 10, 2686-953 Sacavém,  
Portugal

<sup>2</sup> Instituto Português do Mar e da Atmosfera (IPMA), Av. de Brasília, 1449-006 Lisboa,  
Portugal

<sup>3</sup> Centro Interdisciplinar de Investigação Marinha e Ambiental (CIMAR/CIIMAR),  
Universidade do Porto, Porto, Portugal

<sup>4</sup> Departamento de Biologia e Centro de Estudos do Ambiente e do Mar (CESAM),  
Universidade de Aveiro, 3810-193 Aveiro, Portugal

<sup>5</sup> Instituto de Ciências da Vida e Saúde (ICVS), Escola de Ciências da Saúde,  
Universidade do Minho, Campus de Gualtar, 4710-057 Braga, Portugal

<sup>6</sup> Instituto de Bioengenharia e Biociências, Instituto Superior Técnico, Universidade de  
Lisboa, Portugal

\*Corresponding author:

Rita Mendes Godinho

E-mail: [rmgodinho@yahoo.com](mailto:rmgodinho@yahoo.com)

Phone: +351-213027000

Fax : +351-213015

email: [rmgodinho@yahoo.com](mailto:rmgodinho@yahoo.com)

## Abstract

The elemental distributions in *optic tectum* of brains of wild *Liza aurata* a teleost fish captured in polluted and reference coastal areas were assessed quantitatively by nuclear microscopy providing insights into brain vulnerability to metal pollution. Elemental maps enabled to visualize *optic tectum* layers and identify cellular arrangements. Whereas Cl, K and Ca contents identify meninges, the Ca, Fe and Zn concentrations distinguish the underneath grey matter, white matter and inner cellular layers. Exposed animals showed significantly decreased P concentrations and increased contents of Cu, Zn and Ni in all brain structures. These changes highlight homeostasis modification, altered permeability of the blood-brain barrier and suggest risk for neurological toxicity. Our study initiated for the first time an inventory of physiological measures containing images and elemental compositions of brain regions of fish exposed to different environmental conditions. This will help defining total and local brain vulnerability to metals and pollution levels.

**Keywords:** Trace elements mapping; Brain; *Liza aurata*; Environmental exposure neurotoxicity

## 1. Introduction

Fish are key components of the trophic chains and also play an important role signalling water pollution, once they react with great sensitivity to changes in the aquatic systems.<sup>1</sup> Recently brain was pointed as a potential target tissue of environmental metal contamination<sup>2,3,4,5</sup> but the influence of trace elements in fish neurophysiology has been scarcely addressed.<sup>6</sup> The metal imbalance in fish is thought to play a critical role in

1  
2  
3  
4 neurodegeneration and neuronal dysfunctions.<sup>7,8</sup> The health of neuronal tissue is  
5 important in cognitive processes, vision and locomotion among other functions.  
6  
7  
8 Therefore, alterations in brain function due to metal imbalances may endanger not only  
9  
10 the individual but also the population. Physiological measures can provide valuable  
11 indicators for monitoring, implement restoration strategies and improve fisheries  
12 management and conservation. Research in the biology of elements in fish brain may  
13 shed light into potential risks of metal exposure considering population dynamics.  
14  
15  
16  
17  
18

19 To date, there has yet to be a comprehensive, atlas of the distribution and function of  
20 metals in fish brain. Mapping elemental distributions in animal tissues requires  
21 techniques with multi-elemental capabilities, high-spatial resolution and sufficient  
22 sensitivity to detect vestigial concentrations of metals. Nuclear microscopy technique  
23 combines most of these features.<sup>9,10,11</sup> It allows imaging and quantitative determination  
24 of the distribution of elements with sub-cellular resolution, thus enabling to understand  
25 the link between metal localization and function. The nuclear microscopy has been used  
26 for the analysis of thin tissue sections, in both environmental<sup>12,13</sup> and biomedical  
27 research.<sup>14,15,16</sup>  
28  
29  
30  
31  
32  
33  
34  
35  
36  
37  
38

39 We have thus begun providing information on the distribution and functional  
40 significance of metals in the brain of fish *Liza aurata* using nuclear microscopy  
41 mapping. *Liza aurata* is a ubiquitous species in coastal ecosystems that is often used as  
42 a bioindicator of water quality. In this first report results from optic *tectum* region are  
43 described. The optic *tectum* is one of the fundamental components of the vertebrate  
44 brain, existing across the full range of species from hagfish to humans, being considered  
45 a homologue of the mammalian superior *colliculus*. In teleost fish it is greatly expanded  
46 and as been used as study model for the vertebrate species.<sup>17,18,19</sup> Beyond it is  
47  
48  
49  
50  
51  
52  
53  
54  
55  
56  
57  
58  
59  
60

1  
2  
3  
4 considered the main visual centre is involved in a wide variety of activities such as the  
5  
6 goal-directed locomotion.<sup>17</sup>  
7

8  
9 This study evaluates major and trace elemental contents, essential and toxic, and their  
10  
11 compartmentalization in optic lobe structures of *Liza aurata* captured from polluted and  
12  
13 clean areas of a coastal system providing insights into species physiological  
14  
15 requirements and vulnerability to metal toxicity. This is the first multi-elemental  
16  
17 mapping of neuronal tissue of teleost fish.  
18  
19

## 20 21 **2. Experimental**

### 22 **2.1. Sampling area and characterization of fish pollution profile**

23  
24 Native *Liza aurata* individuals were captured at two locations, a polluted and a  
25  
26 reference area, of Aveiro coastal lagoon, in the northwest of Portugal.  
27  
28

29  
30 Laranjo, the polluted area, is an inner and enclosed contaminated basin that has received  
31  
32 effluents from a chloro-alkali plant during around five decades (1950-1994). Its  
33  
34 contamination with Hg has been largely studied<sup>3,5</sup> however this area also presents high  
35  
36 levels of other metals in sediments.<sup>20</sup> São Jacinto, the reference site, situates near the  
37  
38 lagoon entrance, distancing around 10 km from the most contaminated area (Laranjo).  
39

40  
41 Sediment metal concentration from Laranjo were higher than from reference area,  
42  
43 namely: 21  $\mu\text{gg}^{-1}$  Ni, 29  $\mu\text{gg}^{-1}$  Cu, 119  $\mu\text{gg}^{-1}$  Zn and 0.33  $\mu\text{gg}^{-1}$  Cd at Laranjo and 2.4  
44  
45  $\mu\text{gg}^{-1}$  Ni, 14  $\mu\text{gg}^{-1}$  Cu, 2.9  $\mu\text{gg}^{-1}$  Zn and 0.02  $\mu\text{gg}^{-1}$  Cd at S. Jacinto (unpublished data).  
46  
47

48  
49 Liver metal (Ni, Cu, Zn, As, Se, Cd and Pb) concentrations from n=10 fish captured at  
50  
51 the same survey also were significantly different (Wilcoxon Mann-Whitney test,  
52  
53  $p < 0.05$ ) between the two areas, respectively:  $1.7 \pm 0.43 \mu\text{gg}^{-1}$  Ni,  $275 \pm 137 \mu\text{gg}^{-1}$  Cu,  $73$   
54  
55  $\pm 18 \mu\text{gg}^{-1}$  Zn,  $11 \pm 2.7 \mu\text{gg}^{-1}$  As,  $0.6 \pm 0.13 \mu\text{gg}^{-1}$  Cd and  $0.7 \pm 0.25$  Pb for S. Jacinto,  
56  
57  
58  
59  
60

1  
2  
3  
4 and  $3 \pm 0.75 \mu\text{gg}^{-1}\text{Ni}$   $1106 \pm 191 \mu\text{gg}^{-1}\text{Cu}$ ,  $94 \pm 19 \mu\text{gg}^{-1}\text{Zn}$ ,  $14 \pm 2 \mu\text{gg}^{-1}\text{As}$ ,  $0.96 \pm 0.29$   
5  
6  $\mu\text{gg}^{-1}\text{Cd}$  and  $0.60 \pm 0.3 \mu\text{gg}^{-1}\text{Pb}$  for Laranjo (unpublished data). Mercury levels in the  
7  
8 brain, eye wall and lens of fish from the same areas were recently published and pointed  
9  
10 out to significantly higher accumulation at Laranjo than reference area.<sup>5</sup>  
11  
12

## 13 14 15 **2.2. Sampling**

16  
17 Golden grey mullet (*L. aurata*) were collected using a traditional beach-seine net.  
18  
19 Immediately after catching, fish brain was dissected and deep-frozen in liquid nitrogen.  
20  
21 Optical lobe transversal sections of 20  $\mu\text{m}$  were obtained at midbrain level from the  
22  
23 frozen material in a cryo-microtome. The sections were deposited on 1.5  $\mu\text{m}$   
24  
25 polycarbonate foils and freeze-dried before analysis. The cellular integrity was checked  
26  
27 under the light microscope, previous to analysis.  
28  
29  
30  
31  
32

## 33 **2.3. Elemental distribution determination**

34  
35 The samples were examined at the proton microprobe facility of Centro Tecnológico e  
36  
37 Nuclear/IST.<sup>21,22</sup> A proton beam of 2 MeV energy with a current of 100 pA and of 3  $\mu\text{m}$   
38  
39 resolution was used to scan the samples. Particle induced X-ray emission (PIXE),  
40  
41 Rutherford backscattering spectrometry (RBS), and scanning transmission ion  
42  
43 microscopy (STIM) were used simultaneously to obtain morphological and quantitative  
44  
45 elemental distribution data. The PIXE technique is capable of simultaneous  
46  
47 multielementary analysis providing information on both major and trace elements,  
48  
49 although in the conditions used in the this work Hg was not detectable. The RBS  
50  
51 enables the measurement of matrix composition, depth variations and sample  
52  
53 stoichiometry to normalize PIXE spectra for calculation of elemental concentrations.<sup>23</sup>  
54  
55  
56  
57  
58  
59  
60

1  
2  
3  
4 STIM provides measures of areal density variations, and high-resolution images (<0.5  
5  $\mu\text{m}$ ) of the sample morphology.<sup>24</sup> Maps of tissue sections were generated assigning the  
6 various detector signals to a digital X–Y positional coordinate. Selected areas ranging  
7 between approximately 250x250  $\mu\text{m}^2$  and 1000x1000  $\mu\text{m}^2$  were scanned. The relative  
8 amount measured was represented by a colour gradient. Concentration profiles were  
9 produced using point analyses in selected transects across scanned areas.

## 17 **2.4 Data analysis**

18  
19 The combination of PIXE and RBS data was used to quantify elemental concentrations  
20 as described elsewhere.<sup>25</sup> The areal density information obtained through STIM was  
21 used to identify tissue morphology in scanned areas and correlate those details with  
22 elemental distribution obtained by PIXE.<sup>24</sup> Data acquisition and elemental quantitative  
23 analysis were performed using OMDAQ and DAN32 software.<sup>26,23</sup> Elemental  
24 concentration data in the different optic *tectum* regions result from the average of, at  
25 least, five replicates of each point analysis in various sections from 2 fish brains at both  
26 polluted and reference areas. Elemental concentrations of reference and exposed brains  
27 were compared applying Mann-Whitney non-parametric test. Tests were considered  
28 significant when  $p \leq 0.05$ .

## 33 **3. Results**

### 34 **3.1. *Liza aurata* optic *tectum* morphology and elemental mapping**

35  
36 Figure 1 and 2 illustrate how it was possible to characterize and distinguish the different  
37 brain tissues and cellular structures based on areal density and elemental distribution  
38 maps. Figure 1 show a transversal section of the optical lobe of *Liza aurata* from the  
39 reference area. The analysed area of superior optic *tectum* is signed on the optical  
40  
41  
42  
43  
44  
45  
46  
47  
48  
49  
50  
51  
52  
53  
54  
55  
56  
57  
58  
59  
60

1  
2  
3  
4 microscopy photo on the left [Figure 1\_1]. The layered organization could be visualized  
5  
6 using STIM maps of areal mass density variations (Fig.1\_2) and having optical stained  
7  
8 sections as reference. Four main areas were identified from the outer exterior layer: (i)  
9  
10 meninges (M); (ii) peripheral zone of grey matter (PG); (iii) central zone of white matter  
11  
12 (CW); (iv) inner cellular layer (CL). Also the lobular arrangement of optic *tectum* could  
13  
14 be visualized (Fig. 1\_5). The meninges membranes are clearly evidenced in density  
15  
16 maps (Fig. 1\_3 and 1\_4). Below the meninges different density layers of grey and  
17  
18 white matter were distinguished (Fig. 1\_5). The inner cellular layer showed a  
19  
20 characteristic granular-like morphology (Fig. 1\_6).  
21  
22

23  
24 Elemental distribution maps obtained with PIXE also differentiate these four regions  
25  
26 (meninges, grey matter, white matter and cellular layer), as illustrated in Fig. 2 for optic  
27  
28 *tectum* superior layers. The Cl, K and Ca contents identify the outer layer,  
29  
30 corresponding to the meninges (Fig. 2A), whereas Ca, Fe and Zn enabled to distinguish  
31  
32 between deeper layers, such as the peripheral grey and white matter (Fig. 2B). The inner  
33  
34 cellular layer showed a homogeneous distribution for most elements detected as  
35  
36 illustrated for K in Fig. 2C. The granular structure evidenced in the density maps can be  
37  
38 also visualized by Ca distribution. However, the details of both density and Ca images  
39  
40 did not exactly match. Elemental distribution maps are useful to identify the brain  
41  
42 architecture but they only provide qualitative information. To obtain quantitative data  
43  
44 on elemental concentrations, point analyses have to be performed on selected transepts  
45  
46 across the tissue sections<sup>24,25,26</sup>. This procedure enabled to accurately associate  
47  
48 elemental concentrations to the different brain structures and therefore to compare  
49  
50 animals caught at control and polluted areas as described below.  
51  
52  
53  
54  
55  
56  
57  
58  
59  
60

### 3.2. Elemental concentrations in the optic *tectum* of *Liza aurata*

In animals captured in the reference area, the concentrations of P, S and Cl were relatively constant in all brain regions across the optic *tectum* (Fig. 3). The levels of K, Ca, Fe, Cu and Zn were mostly useful to discriminate outer and inner layers (from meninges to the interior cellular layer). Peripheral grey matter regions contrasted to other brain regions by a two-fold higher Fe content ( $41 \pm 8 \mu\text{g/g}$ ). On the other hand, the white matter regions showed the lowest concentrations of Cu and Zn, close to the detection limit (5-8  $\mu\text{g/g}$ ). Higher contents of K, Ca, Cu and Zn were measured in the inner cellular layer and meninges, relative to other brain regions, as can be inferred from Fig. 3.

### 3.3. Vulnerability of brain to environmental pollution

Brain of animals captured in the polluted area showed remarkable concentration differences compared with the brain of ones captured at the reference area (see Fig. 3) namely for P, Ni, Cu and Zn. All analysed optic *tectum* regions of fish from the polluted area were depleted in P and showed an increase of Cu and Zn. The meningeal layer, peripheral grey and central white regions of pollution exposed fish brain showed a ten-fold increase of Cu and Zn concentrations, while in the inner cellular layer smaller changes were observed (see Fig. 3). The most striking alteration found was the presence of Ni in all brain regions of fish from polluted site, contrasting with the fish from the reference site, where Ni was not detected. These alterations were more evident in the meninges and inner cellular layer. In these two regions a 25% increase of Ca concentration was also observed in fish from the polluted site, opposite to the other regions where Ca diminished, although significance was only verified in CW region.

#### 4. Discussion

The meningeal layers cover the teleost central nervous system, give protection and have protein secretion function. They are an interface between the vascular tissue and the cerebrospinal fluid and are active in the blood brain barrier.<sup>27,28</sup> In this context it is relevant the presence of electrolytes and essential trace elements that guarantee the cellular metabolism and neuronal communication.

The central white matter layer contains many fibres, mainly the axons and efferent nerve fibres of cells that originate at grey matter layer. The very low contents of Cu and Zn in the central white matter probably relates to the physiologic characteristics of this brain region. The axon has a reduced metabolic activity compared with the one achieved in the cell body.<sup>29</sup> Consequently higher elemental concentration would be expected in the layers associated with cellular bodies, such as the peripheral grey, containing neuronal cell bodies, fibres and synapses, and the inner cellular layers, mainly composed of neuronal cell bodies. In fact, relevant concentrations of Fe, Cu and Zn were associated with these regions. These three elements are essential to many cellular functions and enzymatic reactions such as protein synthesis, metabolism, and cellular energetics. Prohaska and Bailey<sup>30</sup> reported on high Zn and Cu concentrations in brain compared to other organs of fish highlighting its responsibility in normal central nervous system development and function.

Major changes in elemental contents were observed in the brain of animals from the contaminated Laranjo area. Increasing concentrations of Cl and K in the meninges observed in fish from the polluted area may influence the osmotic potential, altering cell permeability to metals. The enhanced concentrations of S, Fe, Ni, Cu and Zn at the

1  
2  
3  
4 meningeal layers were reflected in different magnitudes, in the underneath layers of  
5  
6 optic *tectum*. Therefore, the meninges metal enrichment suggests a role of this brain  
7  
8 structure in the control of elemental pools and the passage of those elements to and from  
9  
10 blood vessels.<sup>31</sup>

11  
12 The increases of Cu, Zn and Ni contents in optic *tectum* regions reflect the permeability  
13  
14 of the blood-brain barrier for these metals. Copper and Zn have multiple essential  
15  
16 physiological roles and therefore need to be readily available to brain cells. However, an  
17  
18 overload of these elements in the brain tissue may influence metabolism. Copper may  
19  
20 be involved in oxidative pathways with damaging consequences being observed to have  
21  
22 neurological effects.<sup>32</sup> Although deleterious effects associated with Zn are negligible,  
23  
24 since it can be chelated by many proteins and is not involved in oxidative reactions,  
25  
26 exposure to excessive concentrations was observed to cause behavioural alterations in  
27  
28 fish.<sup>33</sup> Nickel was nil in brain tissues of reference area animals. In exposed animals all  
29  
30 brain regions showed increased Ni concentrations indicating a permeability of the  
31  
32 blood-brain barrier to Ni and suggesting risk for neurological toxicity due to this  
33  
34 teratogenic element. A well-known metal detoxification strategy consists of inducing  
35  
36 metallothioneins, proteins to which several metals and metalloids have a high  
37  
38 affinity.<sup>34,35</sup> However, a similar role for fish brain metallothioneins has not been  
39  
40 established yet, results have been reported to be species, metal and condition  
41  
42 specific.<sup>36,37,38</sup> Increased sulphur concentration in cellular layer of exposed fish may be  
43  
44 related with enhanced protein content suggesting high relevance of further studies on  
45  
46 this matter.  
47  
48  
49  
50  
51

52  
53 The Ca decrease in central white mater region (axons and efferent nerve fibres) and Cl  
54  
55 increase in cellular layers (cell bodies) may have physiological effects in neuronal  
56  
57  
58  
59  
60

1  
2  
3  
4 function. However, no significant changes of K were observed in our study, opposite to  
5 reported studies on fish brain exposed to pesticides and cadmium.<sup>39,40</sup>  
6  
7

8 The decrease of P concentrations observed in exposed organisms may indicate a down  
9 regulation of metabolic activity. The lower availability or retention of P may have  
10 drastic consequences as neuronal activity is highly dependent on ATP consumption.<sup>41</sup>  
11  
12

13 This may be caused by excess of Fe, Ni and Cu as these elements can modulate  
14 oxidation-reduction reactions, influence or impair metabolic pathways, transport across  
15 cell membranes, axonal transport, and metal-responsive transcription factors, among  
16 other features.<sup>42</sup>  
17  
18  
19  
20  
21  
22

23 Further data is required to link these elemental concentration changes to specific cellular  
24 environments. In this context, detailed information of the reference brain would be  
25 useful. Both elemental maps of multiple planes and detailed elemental distribution at  
26 cellular level would be helpful to interpret the role of the elements in brain physiology  
27 and the effects of their concentration changes in fish behaviour and disease.  
28  
29  
30  
31  
32  
33  
34  
35  
36

#### 37 **4. Conclusion**

38 To our knowledge, this study was the first performing elemental mapping and initiating  
39 a quantitative elemental inventory of neuronal tissue of teleost fish.  
40  
41  
42

43 Nuclear microscopy mapping and quantification of elements proved to be appropriate to  
44 spatially resolve brain morphological structures and detect diminutive variations of  
45 elemental concentrations. In the reference brain elemental signatures characterized  
46 different brain structures enabling to associate these signatures with the tissues  
47 physiological roles. Whereas Cl, K and Ca contents identify meninges, the Ca, Fe and  
48 Zn distinguish optical *tectum* layers. Brains of exposed animals showed altered  
49  
50  
51  
52  
53  
54  
55  
56  
57  
58  
59  
60

1  
2  
3  
4 elemental concentrations in the meninges and underneath optic *tectum* layers. These  
5  
6 changes highlight homeostasis modification, altered permeability of the blood-brain  
7  
8 barrier and suggest risk for neurological toxicity and behaviour alteration.  
9

10 The elemental distributions of optic *tectum* of *L. aurata* brain reflected environmental  
11  
12 burden, which can be useful for biomonitoring. In addition, cataloguing fish brain will  
13  
14 have a significant impact in estimating neuronal health effects and will pave the way to  
15  
16 further neurotoxicity studies. This is of particular relevance as teleost fish has been used  
17  
18 as a model to study the central nervous system of vertebrate species  
19  
20  
21  
22  
23

#### 24 **Acknowledgments**

25  
26 R.M. Godinho, P. Pereira and J. Raimundo work have as been supported by “Fundação  
27  
28 para a Ciência e a Tecnologia” (FCT), through Grants N° SFRH\_BPD\_47473\_2008,  
29  
30 SFRH/BPD/69563/2010 and SFRH/BPD/91498/2012 respectively. We express  
31  
32 appreciation for the support from the Research project financed by FCT PTDC/AAG-  
33  
34 REC/ 2488/2012 (NEUTOXMER — Neurotoxicity of mercury in fish and association  
35  
36 with morphofunctional brain alterations and behaviour shifts).  
37  
38  
39  
40  
41

#### 42 **References**

- 43  
44 1. R. Van der Oost, J. Beyer and N.P.E. Vermeulen, Environ. Toxicol. Pharmacol. 13,  
45  
46 2003, 57-149  
47  
48 2. F.R. de la Torre, L. Ferrara and A. Salibia, Comparative Biochemistry and  
49  
50 Physiology Part C 131, 2002, 271–280.  
51  
52  
53 3. C.L. Mieiro, M. Pacheco, M.E. Pereira, A.C. Duarte, J. Environ. Monitor. 11, 2009,  
54  
55 1004-1011.  
56  
57  
58  
59  
60

- 1  
2  
3  
4 4. R. Siscar, A. Torreblanca, A. Palanques and M. Solé, *Marine Pollution Bulletin* 77,  
5  
6 2013, 90–99.  
7
- 8  
9 5. P. Pereira, J. Raimundo, O. Araújo, J. Canário, A. Almeida, M. Pacheco, *Sci. Total*  
10  
11 *Environ.* 494, 2014, 290-298. doi:0.1016/j.scitotenv.2014.07.008.  
12
- 13 6. M. H.G. Berntssen, A. Aatland and R. D. Handy, *Aquatic Toxicology* 65, 2003, 55-  
14  
15 72.  
16
- 17 7. P.A. Lopes, T. Pinheiro, M.C. Santos, M.L. Mathias, M.J. Collares-Pereira, A.M.  
18  
19 *Viegas-Crespo*, *Sci. Total. Environ.* 280, 2001, 153-163.  
20
- 21 8. R. Ortega, P. Cloetens, G. Devès, A. Carmona and S. Bohic, *PLoS ONE* 2(9), 2007,  
22  
23 e925.  
24
- 25 9. R. Ortega, G. Devés and A. Carmona, *J. R. Soc. Interface* 6, 2009, S649-S658.  
26  
27
- 28 10. R. Rajendran, R. Minqin, J.A. Ronald, B.K. Rutt, B. Halliwell and F. Watt, *Free*  
29  
30 *Radical Biology and Medicine* 53, 2012, 1675–1679.  
31
- 32 11. M.D. Ynsa, R. Minquin, R. Rajendran, T. Pinheiro and F. Watt, *Microsc. Microanal.*  
33  
34 18, 2012, 1060–1066. doi:10.1017/S1431927612001547.  
35  
36
- 37 12. R.M. Godinho, J. Raimundo, C. Vale, B. Anes, P. Brito, L. Alves and T. Pinheiro,  
38  
39 *Nucl Instr Meth B* 306, 2013, 150-152.  
40
- 41 13. R.M. Godinho, M.T. Cabrita, L. Alves and T. Pinheiro, *Metallomics* 20, 2014,  
42  
43 1626-31. doi: 10.1039/c4mt00105b.  
44
- 45 14. R. Siegele, N.R. Howell, P.D. Callaghan and Z. Pastuovic, *Nuclear Instruments and*  
46  
47 *Methods in Physics Research B* 306, 2013, 125–128.  
48
- 49 15. M.J. Hackett, R. Siegele, F. El-Assaad, J.A. McQuillan, J.B. Aitken, E.A. Carter,  
50  
51 *G.E. Grau, N.H. Hunt, D. Cohen and P.A. Lay*, *Nuclear Instruments and Methods in*  
52  
53 *Physics Research B* 269, 2011, 2260–2263.  
54  
55  
56  
57  
58  
59  
60

- 1  
2  
3  
4 16. T. Pinheiro, R. Silva, R. Fleming, A. Gonçalves, M.A. Barreiros, J.N. Silva, P  
5  
6 Morlière, R. Santus and P. Filipe, *Acta Derm. Venereol.* 94, 2014, 14-19.  
7  
8  
9 17. K. Saitoh, A. Ménard and S. Grillner, *J. Neurophysiol.* 97, 2007, 3093-3108.  
10  
11 18. R. Vargas, Ip. Jóhannesdóttir, B. Sigurgeirsson, H. Borsteinsson and K. Æ. Karlsson  
12  
13 *Advan in Physiol Edu* 35, 2011, 188-196.  
14  
15 19. L.A. O'Connell, M.R. Fontenot and H.A. Hofmann, *J. Chem. Neuroanat.* 47, 2013,  
16  
17 106-115.  
18  
19 20. V. Martins, C. Yamashita, S.H.M. Sousa, P. Martins, L.L.M. Laut, R.C.L. Figueira,  
20  
21 M.M. Mahiques, E.F. Silva, J.M.A. Dias and F. Rocha, *Journal of Iberian Geology* 37,  
22  
23 2011, 231-246. doi: 10.5209/rev\_JIGE.2011.v37.n2.10.  
24  
25 21. L.C. Alves, M.B.H. Breese, E. Alves, A. Paul, M.R. Silva, M.F. Silva and J.C.  
26  
27 Soares, *Nucl. Instr. Meth. B*, 2000, 161, 334-338.  
28  
29 22. A. Veríssimo, L.C. Alves, P. Filipe, J.N. Silva, R. Silva, M.D. Ynsa, E. Gontier,  
30  
31 J.M. Pallon and T. Pinheiro, *Microsc. Res. Tech.* 70, 2007, 302-9.  
32  
33 23. G.W. Grime, *Nuclear Instruments and Methods in Physics Research Section B*  
34  
35 109/110, 1996, 170-174.  
36  
37 24. P. Aguer, L.C. Alves, Ph. Barbereth, E. Gontier, S. Incerti, C. Michelet-Habchi, Zs.  
38  
39 Kertész, A.Z. Kiss, P. Moretto, J. Pallon, T. Pinheiro, J.E. Surlève-Bazeille, Z. Szikszai,  
40  
41 A. Veríssimo and M.D. Ynsa. *Nucl Instrum Meth B* 231, 2005, 292-299.  
42  
43 25. G.W. Grime and M. Dawson, *Nucl. Instr. Meth. B* 104, 1995, 107-113.  
44  
45 26. G.W. Grime and M. Dawson, *Nucl. Instr. Meth. B* 89, 1994, 223-228.  
46  
47 27. A. Königstorfer, S. Sterrer and W. Hoffmann, *Cell. Tissue Res.* 261, 1990, 59-64.  
48  
49 28. H.J. Caruncho, S.P. Pinto and R. Anadon, *J. Submicrosc. Cytol. Pathol.* 25, 1993,  
50  
51 97-406.  
52  
53  
54  
55  
56  
57  
58  
59  
60

- 1  
2  
3  
4 29. M. Bélanger, I. Allaman and P.J. Magistretti, *Cell Metabolism* 14, 2011, 725-738.  
5  
6 doi: 10.1016/j.cmet.2011.08.016.  
7  
8  
9 30. J.R. Prohaska and W.R. Bailey, *Proc. Soc. Exp. Biol. Med.* 210, 1995, 107-16.  
10  
11 31. W. Zheng, M. Aschner and J.F. Ghersi-Egea, *Toxicology and Applied*  
12  
13 *Pharmacology* 192, 2003, 1–11.  
14  
15 32. C.D. Ezeonyejiaku, M.O. Obiakor and C.O. Ezenwelu, *Online J. Anim. Feed Res.* 1,  
16  
17 2011, 130-134.  
18  
19 33. N.N. Singh, V.K. Das and A.K. Srivastava, *Zoologica Poloniae* 47, 2002, 21-36.  
20  
21 34. G. Roesijadi, *Aquat. Toxic.* 22, 1992, 81-114.  
22  
23 35. A. Viarengo and J.A. Nott, *Comp. Biochem. Physiol. C* 104, 1993, 355-372.  
24  
25 36. F. Atif, M. Kaur, R.A. Ansari and S. Raisuddin, *J. Biochem. Mol. Toxicol.* 22,  
26  
27 2008, 202-208. doi: 10.1002/jbt.20230.  
28  
29 37. C.L. Mieiro, L. Bervoets, S. Joosen, R. Blust, A.C. Duarte, M.E. Pereira and M.  
30  
31 Pacheco, *Chemosphere* 85, 2011, 114-21. doi: 10.1016/j.chemosphere.2011.05.034.  
32  
33 38. M. Sevcikova, H. Modra, K. Kruzikova, O. Zitka, D. Hynek, V. Adam, O.  
34  
35 Celechovska, R. Kizek and Z. Svobodova, *Int. J. Electrochem. Sci.* 8, 2013, 1650-1663.  
36  
37 39. A. Larsson, B.E. Bengtsson and C. Haux, *Aquat. Toxicol.* 1, 1981, 19-35.  
38  
39 40. Swarnlata, Ph.D. Thesis, Avadh University, Faizabad, India, 1995.  
40  
41 41. M. Vos, E. Lauwers and P. Verstreken, *Front. Synaptic Neurosci.* 2, 2011, 139. doi:  
42  
43 10.3389/fnsyn.2010.00139.  
44  
45 42. J.C. Rutherford and A.J. Bird, *Eukaryot Cell.* 3, 2004, 1–13. doi: 10.1128/EC.3.1.1-  
46  
47 13.2004.  
48  
49  
50  
51  
52  
53  
54  
55  
56  
57  
58  
59  
60

**Figure captions**

**Fig 1.** Transversal section of the *Liza aurata* brain at midbrain level. 1) Optical microscopy image on the left identifies the region of the superior optic *tectum* analysed by nuclear microscopy (rectangle). 2) Nuclear microscopy areal mass density (STIM) map of the scanned region identifying optic *tectum* layers. 3), 4), 5) and 6) Zoomed STIM maps of on the different layers: M – Meningeal layers; PG – peripheral zone of grey matter; CW – central zone of white matter; CL – inner cellular layer. Density gradient represented by a dynamic colour scale: high density - white, to low density – black. Horizontal line denotes 100  $\mu\text{m}$

**Fig 2.** Elemental distribution in the superior optic *tectum* of the brain of *Liza aurata*. A- Meninges layer. B- Grey and white matter layers. C- Cellular layers. Areal mass density (STIM), on the left, and elemental distribution maps obtained by PIXE on the right: M – Meningeal layers; PG – peripheral zone of grey matter; CW – central zone of white matter; CL – inner cellular layer. Density and amount gradient represented by a dynamic colour scale: low – black/ blue to high – white/ red. Horizontal line denotes 100  $\mu\text{m}$

**Fig 3** Elemental concentrations (expressed as mean and standard deviation) in the different layers, from the outer to the interior, of optic *tectum* of *Liza aurata* captured in the reference (white bars) and polluted site (black bars). M – Meningeal layers; PG – peripheral zone of grey matter; CW – central zone of white matter; CL – inner cellular layer. “nd” means not detected; \* indicates significant difference to controls ( $p < 0.05$ )

**Graphical abstract**

Elemental mapping of fish brain exposed to metal pollution revealed altered elemental concentrations that highlight homeostasis modification, altered permeability of the blood-brain barrier and risk for neurological toxicity and behaviour impairments

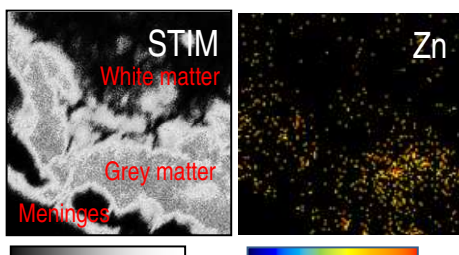
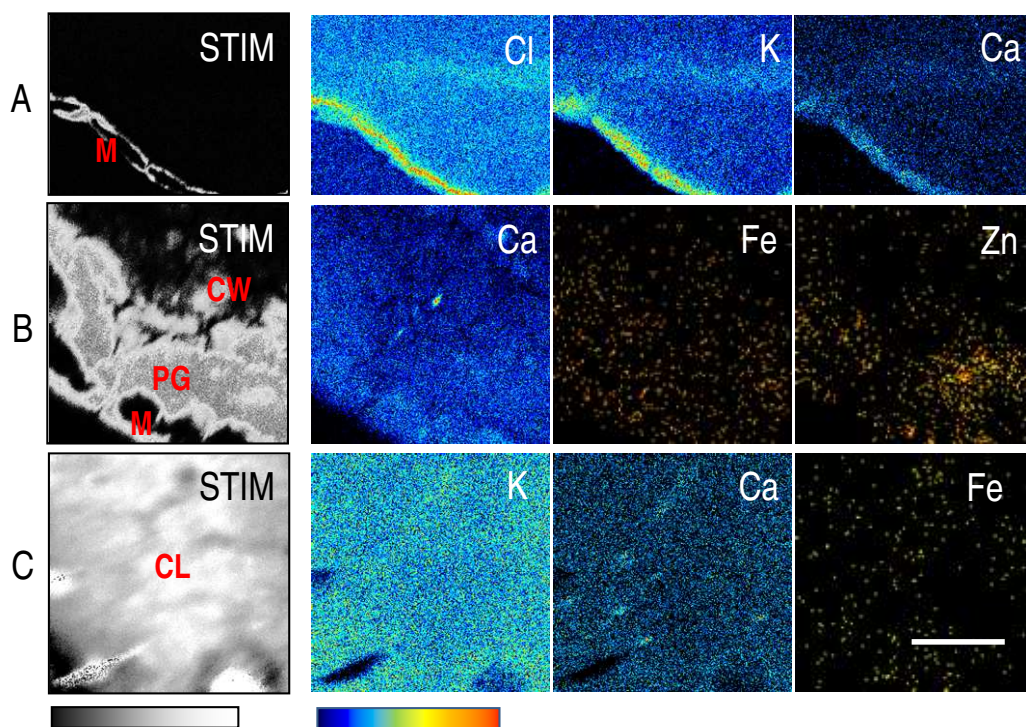


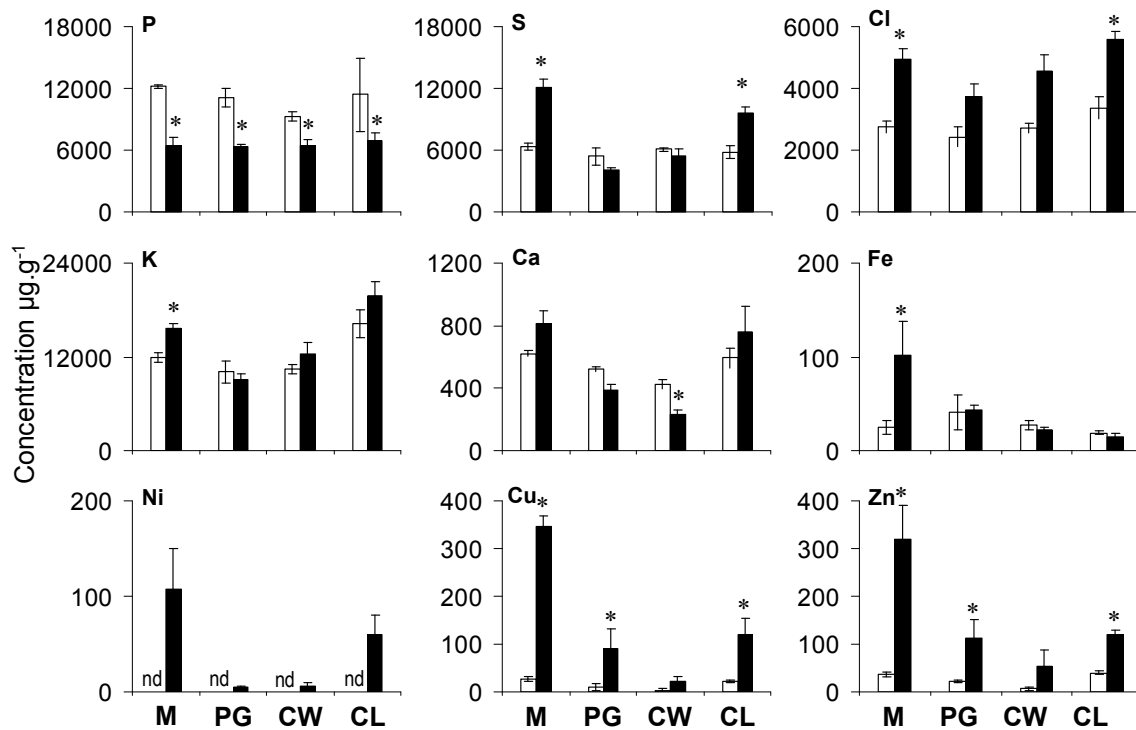


Figure 2



1  
2  
3  
4  
5  
6  
7  
8  
9  
10  
11  
12  
13  
14  
15  
16  
17  
18  
19  
20  
21  
22  
23  
24  
25  
26  
27  
28  
29  
30  
31  
32  
33  
34  
35  
36  
37  
38  
39  
40  
41  
42  
43  
44  
45  
46  
47  
48  
49  
50  
51  
52  
53  
54  
55  
56  
57  
58  
59  
60

Figure 3



1  
2  
3  
4  
5  
6  
7  
8  
9  
10  
11  
12  
13  
14  
15  
16  
17  
18  
19  
20  
21  
22  
23  
24  
25  
26  
27  
28  
29  
30  
31  
32  
33  
34  
35  
36  
37  
38  
39  
40  
41  
42  
43  
44  
45  
46  
47  
48  
49  
50  
51  
52  
53  
54  
55  
56  
57  
58  
59  
60